Giant resonant photoemission at the Mn $2p \rightarrow 3d$ absorption threshold of $Cd_{1-x}Mn_xTe$

L. Sangaletti,[1] S. Pagliara,[1] F. Parmigiani,[1] A. Goldoni,[2] L. Floreano,[3] A. Morgante,[3] and V. Aguekian[4]
[1]*Istituto Nazionale per la Fisica della Materia, Dipartimento di Matematica e Fisica, Università Cattolica del Sacro Cuore, Via dei Musei 41, 25121 Brescia, Italy*
[2]*Sincrotrone Trieste S.C.p.A., S.S. 14 Km 163.5, in Area Science Park, 34012 Trieste, Italy*
[3]*Laboratorio TASC-INFM, Basovizza s.s. 14 Km 163.5, I-34012 Trieste, Italy*
[4]*Solid State Physics Department, V. Fock Institute of Physics, Saint-Petersburg State University, Petrodvoretz, 198904 S.-Petersburg, Russia*
(Received 2 October 2002; revised manuscript received 31 March 2003; published 10 June 2003)

Resonant photoemission spectroscopy data from $Cd_{1-x}Mn_xTe$ single crystals are presented. A strong resonant behavior, related to the Raman-Auger decay channel arising from the creation of the Mn $2p$ core hole, is detected for states in the valence-band region at the Mn $2p \rightarrow 3d$ absorption threshold. The transition from the resonating Raman-Auger to the weak, normal Auger emission is shown to occur well above the main absorption edge. This effect is ascribed to the presence of a manifold of localized states arising from the Mn $2p \rightarrow 3d$ Coulomb and exchange interaction, which prevents the delocalization in the intermediate state of the autoionization process.

DOI: 10.1103/PhysRevB.67.233201 PACS number(s): 79.60.−i, 78.70.Dm, 75.50.Pp, 71.27.+a

Recent advances in the search of new materials for spintronics have prompted a reconsideration of photoelectron spectroscopies for the study of the contribution of magnetic ions to the spectral weight in the valence-band region. In particular, the ferromagnetic $Ga_{1-x}Mn_xAs$ and $In_{1-x}Mn_xAs$ semiconductors and the $Zn_{1-x}Mn_xO$ oxide have attracted particular attention from a spectroscopic point of view, and recent experiments have been reported on resonant photoemission (RESPES) at the Mn $3p \rightarrow 3d$ absorption edge of these compounds.[1–4] These studies are rooted in earlier works,[5,6] which were aimed at identifying the Mn $3d$ spectral weight in the valence-band photoemission spectrum of single crystals of the $Cd_{1-x}Mn_xTe$ diluted magnetic semiconductor (DMS). The photoemission of d electrons from $3d$ transition metals and their compounds is strongly enhanced when the energy of the incoming photon is just enough to excite an np electron ($n=2,3$) to an unoccupied $3d$ level, leading to a process called resonant photoemission. This effect is interpreted as due to a process where an np electron in the initial state is first excited to an empty $3d$ level, forming a tighly bound (np,$3d$) intermediate state. This intermediate state may decay via autoionization, yielding a final state identical to that obtained by the direct photoemission process. For Mn $3d$ electrons the resonance arises when an interference between the direct photoemission channel ($np^6 3d^5 + h\nu \rightarrow np^6 3d^4 e_f$) and the Mn $np \rightarrow 3d$ excitation followed by a Coster-Kronig decay $np^6 3d^5 + h\nu \rightarrow np^5 3d^6 \rightarrow np^6 3d^4 e_f$) occurs. Interference effects can be handled within the Fano formalism.[7,8] The condition for interference to occur is the coherence between the direct and indirect emission channels. The loss of coherence can be due to delocalization of the $3d$ electron in the intermediate state, which produces an energy difference between the final states of the two channels.

When RESPES experiments are carried out across the $2p \rightarrow 3d$ absorption threshold in $3d$ transition-metal compounds, a dramatic enhancement of the electron emission is observed (giant resonance),[9,10] much larger than that observed at the $3p \rightarrow 3d$ threshold. In giant resonance the de-excitation channel—i.e., the photoabsorption process followed by a Coster-Kronig decay—overwhelms the direct photoemission channel. Therefore, the interference effects between the two channels are weaker than in the case of $3p \rightarrow 3d$ absorption.

To the best of our knowledge, resonant photoemission experiments on the Mn $2p \rightarrow 3d$ absorption threshold of diluted magnetic semiconductors have been so far virtually neglected, since all experiments have been performed at the Mn $3p \rightarrow 3d$ absorption threshold. Only the parent MnTe compound[11] has been studied with RESPES at the Mn $2p \rightarrow 3d$ threshold. The aim of the present study is to probe the giant resonance at the Mn $2p \rightarrow 3d$ threshold of single crystal $Cd_{1-x}Mn_xTe$ ($x=0.45$) DMS and to track the transition from the Raman-Auger to normal Auger regime.

The measurements have been performed at the INFM ALOISA synchrotron beamline in Trieste (Italy). For this experiment $Cd_{1-x}Mn_xTe$ single crystals grown with the Bridgman method have been used. The photoemission data were collected in ultra-high vacuum at a base pressure of 1×10^{-10} torr. The crystal surface was prepared by repeated cycles of Ar ion sputtering at 1 keV beam energy and annealing at 320 °C until a clear reflection high-energy electron diffraction (RHEED) image could be detected. Moreover, we also checked the surface composition by collecting x-ray photoemission spectroscopy (XPS) spectra of Cd $3d$, Te $3d$, and Mn $2p$ core levels. We noticed that the sputtering procedure produced Cd-poor surfaces with a prevailing Mn weight, whereas after the annealing process the Cd weight was restored to the expected values. Resonant photoemission and absorption measurements have been taken in transverse-electric polarization at a grazing angle of about 8°. The beamline has been operated between 600 and 700 eV at a resolving power of about 3000 with a photon flux of $0.5–1 \times 10^{12}$ photon/sec.[12] The electron analyzer has been used in normal emission and with a fixed energy resolution of 850 meV, thus yielding an overall resolution better than 1 eV. A channeltron has been used to measure the total electron yield for the absorption spectra.

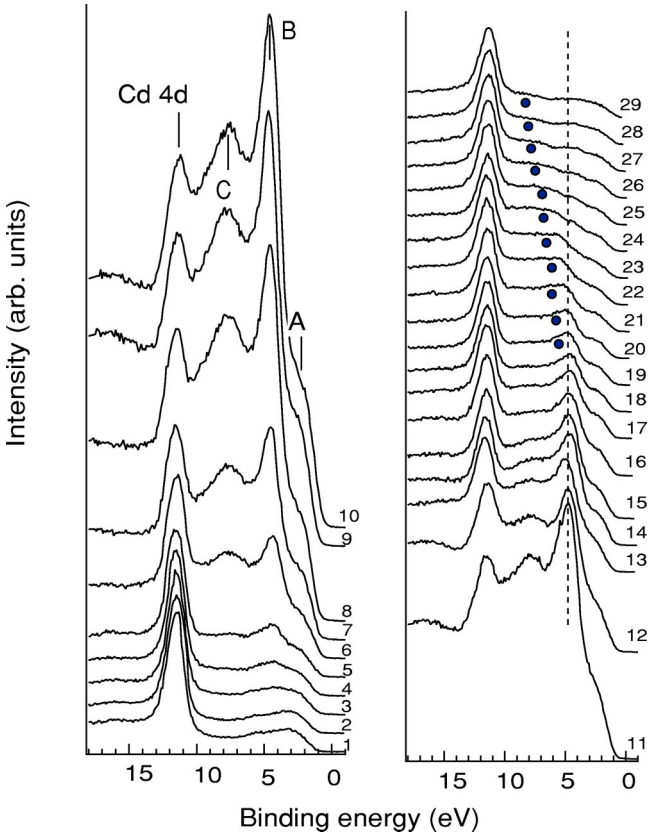

FIG. 1. Resonant valence-band spectra collected with photon energies across the Mn $2p \rightarrow 3d$ absorption threshold. The photon energies are labeled by numbers which correspond to the points indicated on the Mn $2p$ XAS curve shown in Fig. 2. The black dots indicate the normal Auger emission which is found to disperse on the BE scale. The dashed line is drawn as a reference for the non-dispersing Raman-like emission.

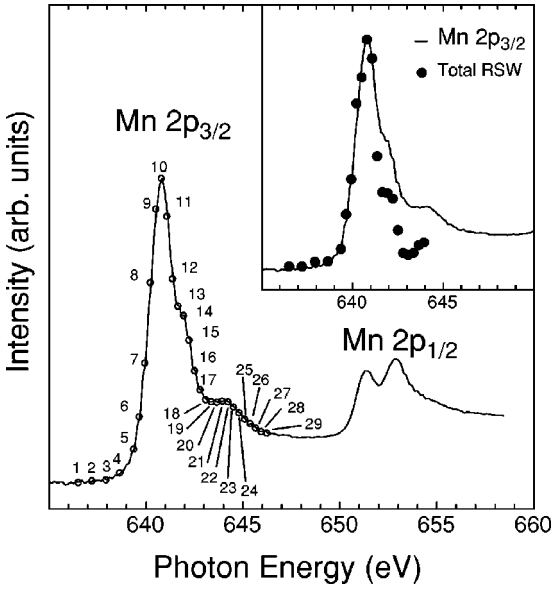

FIG. 2. Mn $2p_{3/2}$ and Mn $2p_{1/2}$ absorption lines of the $Cd_{0.55}Mn_{0.45}Te$ single crystal. The numbers indicate the photon energies at which the photoemission spectra of Fig. 1 were collected. Inset: total resonating spectral weight (RSW) vs photon energy obtained from the RESPES spectra after that the polynomial background, the off-resonance spectrum, and the Cd $4d$ emission have been subtracted. The thin line is the XAS spectrum.

In Fig. 1 the resonant valence-band spectra collected with photon energies across the Mn $2p \rightarrow 3d$ absorption threshold are shown. At a binding energy (BE) of about 11.5 eV the Cd $4d$ shallow core levels can be detected; the intensity of this structure is constant with the photon energy while the intensity of the valence band in the range 2–10 eV strongly increases. The Cd $4d$ emission has been used to normalize the spectra and was taken as a reference for aligning the spectra to a common BE's scale, along with the Te $4d_{5/2}$ core level emission at 42 eV, not shown in the present data. The photon energies are labeled by numbers which correspond to the points indicated on the Mn $2p$ x-ray absorption spectroscopy (XAS) curve shown in Fig. 2.

In Fig. 2(a), both the $2p_{3/2}$ (L_3) and the $2p_{1/2}$ (L_2) lines of the Mn $2p$ absorption spectrum are clearly detectable. Both lines show a fine structure which is ascribed to multiplet effects arising from the Coulomb and exchange interactions between the Mn $2p$ core hole and the Mn open $3d$ shell electrons. This absorption profile is quite similar to that measured for the Mn $2p$ thresholds in other DMS compounds,[13,14] where Mn is tetrahedrally coordinated with the ligand ions. As can be observed in Fig. 1, the resonance of the photoemission spectrum has its maximum at about 640.5 eV (spectrum No. 10). At resonance, three features can be clearly detected. They are labeled as A, B, and C in Fig. 1. At first sight, these features have a constant binding energy and none of them shows an energy dispersion. However, in order to confirm this behavior we had to carry out a data analysis on the rough spectra. The main purpose of the analysis was to identify the spectral profile of the resonating features, track their energy dependence on photon energy, and find out the expected normal Auger emission for photon energies above the absorption threshold. The discussion of our results is based on two issues. The first is related to the deconvolution of the resonating spectral weight in the valence band, while the second is related to the transition from the Raman-Auger to the normal Auger emission.

In order to extract the resonating spectral weight from the valence band data, we have followed a procedure recently applied to the analysis of RESPES at the Cu $2p \rightarrow 3d$ threshold of $CuGeO_3$.[15]

In Fig. 3 an example of the data analysis is shown for the spectrum collected at $h\nu = 640.5$ eV photon energy. The background is subtracted from the valence-band spectrum by using a polynomial function. Four Gaussians are introduced to fit Cd $4d$ and the valence-band emission: one for the Cd shallow core level and three for the resonant valence band [Fig. 3(a)]. The peak intensity of the Cd $4d$ emission was maintained fixed, since the Cd $4d$ photoemission cross section at these energies can be considered constant.[16] The use of three Gaussians for the valence band (VB) is based on the identification of the resonating features of Fig. 1, where the three A, B, and C peaks are clearly detectable. Once the background has been subtracted, one is left with the photoemission spectrum that can be used to extract the pure reso-

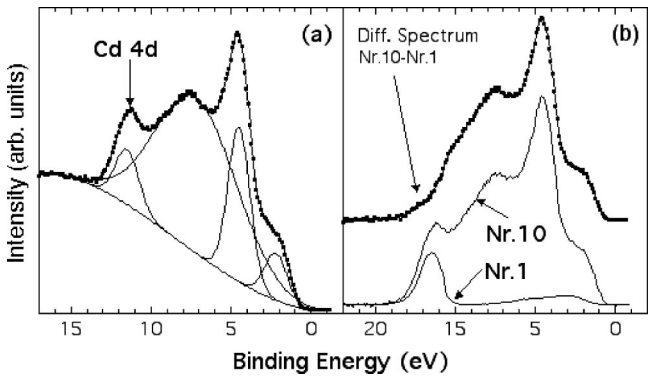

FIG. 3. Example of the data analysis. (a) The background is subtracted from the valence-band spectrum by using a polynomial function. (b) Resonant (No. 10 in Fig. 1) and off-resonance (No. 1 in Fig. 1) spectra after background subtraction. The topmost spectrum represents the pure resonant contribution resulting from the subtraction of the off-resonance from the resonant spectrum.

nant contribution. This contribution is obtained by subtracting from each spectrum the off-resonance spectrum collected at $h\nu = 636.5$ eV (No. 1 in Fig. 1), as shown in Fig. 3(b) for the spectrum collected at 640.5 eV (No. 10 in Fig. 1). In this way, for each photon energy we have been able to estimate the total resonating weight by summing up the area of the A, B, and C Gaussian peaks.

The three spectral features we have identified at the Mn $2p \rightarrow 3d$ resonance have a counterpart in the RESPES study carried out at the Mn $3p \rightarrow 3d$ absorption threshold, as well as in the related impurity cluster calculations of the Mn $3d$ spectral weight proposed by Mizokawa and Fujimori in several photoemission studies of DMS's.[6,17] The identification of $3d^4$ satellites in the Mn $3d$ photoemission spectra of $Cd_{1-x}Mn_xTe$ alloys has been the subject of several experimental and theoretical studies in the past.[6,17–19] When a photoelectron is emitted from the Mn $3d$ orbitals in the ground state, several $3d^4$ configurations may arise, due to multiplet (Coulomb and exchange) splitting.

In addition to multiplet splitting, also Te $5p \rightarrow$ Mn $3d$ charge transfer configurations must be accounted for in the configuration interaction (CI) model for both initial and final states of the photoemission process. Therefore hybridization among charge transfer ($3d^5\underline{L}$) and ionic ($3d^4$) configurations introduces a further redistribution of the spectral weight in the final state. In Ref. 17 impurity cluster CI calculations on $Cd_{1-x}Mn_xTe$ are presented. The calculated Mn $3d$ spectral weight shows a manifold of states which yields three main features, separated by about 3 eV from each other, in agreement with the experimental resonant photoemission data collected at the Mn $3p \rightarrow 3d$ absorption threshold.[6,18] Indeed, by subtracting from the on-resonance spectrum (collected at 49.5 eV photon energy) the VB spectrum collected far from the absorption threshold, it was possible to evidence the resonant contribution of the Mn $3d$ states. Three features resulted from the subtraction: one in the 0–2.5 eV energy range, one at about 3.4 eV, and another broad feature in the 5–9 eV energy range. They correspond to peaks A, B, and C detected in the present data.

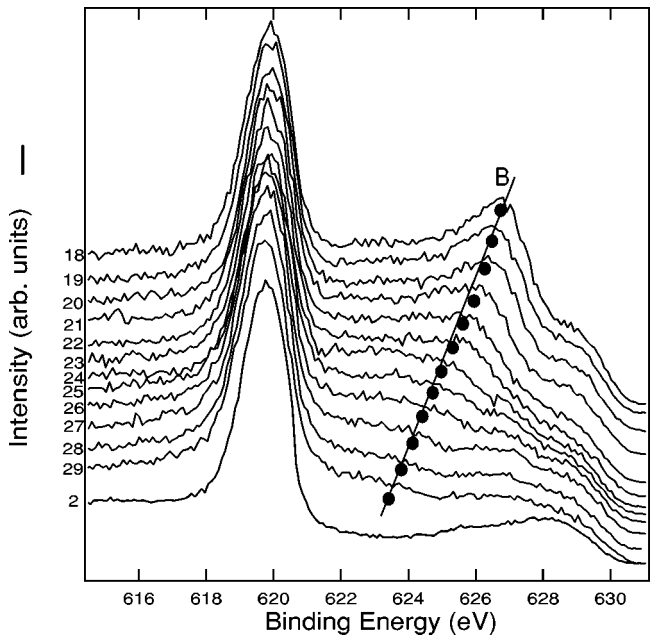

FIG. 4. Detail of the valence-band region with photoemission spectra collected at photon energies above the main line of the absorption spectrum (spectra Nos. 18–29). The bottom spectrum is spectrum No. 1. The dots indicate the normal Auger emission. The line through the dots is drawn as a guide for the eye.

In the inset of Fig. 2 the total intensity of the resonating spectral weight (RSW) against the photon energies is shown, along with the XAS spectrum. The integrated intensity closely reproduces the XAS spectrum with the three structures at about $h\nu = 640.5$, 642, and 644 eV, characteristic of the Mn $2p_{3/2}$ absorption. When the integrated intensity is decomposed into the three A, B, and C components resulting from the data fitting, the constant-initial-state (CIS) profile characteristic of each band—not shown here—closely resembles that extracted from the integrated intensity of the resonanting spectral weight. Therefore, differences between the CIS profiles are not detectable, apart from a scaling factor due to extent of the resonance effect of each single (A, B, or C) structure.

Due to the large number of states, with different symmetry of the $3d^4$ configurations contributing to each of the three A, B, and C bands, according to the calculation results,[17] it is not possible to relate any of the three bands to a well-defined E_g or T_{2g} symmetry of the $3d^4$ final-state configurations. Moreover, there is not a direct relationship between the weight of the $3d^{n-1}$ configuration ($3d^4$, in the present case) in the final state and the extent of the resonance, as found in the case of Cu^{2+} compounds.[15] The valence band resonates not only where the $3d^4$ configuration presents a larger weight (i.e., in the region where the C band is detected), but also where the $3d^5\underline{L}$ configurations mainly contribute (A and B bands) which indicates that resonant photoemission involving more than two holes in the final state may lead to a rather complicated behavior that cannot be directly related to the spectral weight distribution of the $3d^{n-1}$ configurations.

In the resonant spectra taken above 642.5 eV photon energy, in spite of the low intensity of the normal Auger chan-

nel, we have been able to observe the $L_{2,3}M_{4,5}M_{4,5}$ Auger emission, not clearly detectable in the experimental RESPES spectra collected at the Mn $3p_{3/2}$ absorption edge.[6] In Fig. 4 the spectra taken at $h\nu$ ranging from 642.5 to 646 eV (Nos. 18–29) are shown, along with the off-resonant spectrum (No. 1). It is evident that the energy of the B band shows a dispersive behavior on the BE's scale which is characteristic of the normal Auger, i.e., incoherent, emission, expected above the resonance threshold.

The transition from the Raman-Auger to normal Auger regime may be affected by the presence of the multiplet structure. It is possible that when multiplet structures which arise from interatomic Coulomb and exchange interactions and yield fairly localized electronic states are present, the dominant channel is the Raman-Auger emission and therefore the resonant valence band shows a constant binding energy behavior. Only with photon energies well above the main line of the Mn $2p_{3/2}$ multiplet spectrum can the electron delocalize and the Auger channel appear, as shown in Fig. 4, where a broad feature that shows a dispersive behavior versus the BE's is pointed out.

The localization of Mn electrons in Mn ultrathin layers has been recently discussed[20] by analyzing the slope of the BE's versus photon energy curve for several Auger channels. A slope significantly different from one was found for the strong Mn $2p3p3d$ emission. This was ascribed to a mixture of Raman and Auger behavior above threshold induced by localization of the intermediate state. In our case, the straight line in Fig. 4 has only a qualitative value and should be regarded as a guide for the eye, the Auger emission being rather broad and structured. Therefore, at the present stage we cannot extract quantitative information on the BE's versus photon energy slopes for the $Cd_{1-x}Mn_xTe$ system, until further work is carried out by comparing the behavior of the Mn $2p3d3d$ Auger emission in the valence-band region with that of the Mn $2p3p3d$ Auger emission at higher energies.

In conclusion, the transition from a coherent, Raman-like to an incoherent, normal Auger regime has been tracked. The resonance effect is still contributing above the photon energy of the absorption main peak, and the integrated intensity of the RSW reproduces the multiplet features of the absorption profile. This is ascribed to the localization of the intermediate state which can be favored by the extent of the manifold of states arising from multiplet splitting. The enhancement of the resonance in the valence-band region is larger than that detectable at the Mn $3p \rightarrow 3d$ threshold. This finding suggests that, especially in the case of the new ferromagnetic DMS's, where impurities with a concentration x smaller than 0.1 have been reported,[2–4] RESPES experiments may profit from the enhancement at the $2p$ threshold to probe the spectral weight of the magnetic ions.

L.S. and S.P. acknowledge financial support from the INFM-LdS project. S.P. also gratefully acknowledges C. Fadley for stimulating discussions during the School on Synchrotron Radiation held at ICTP in Trieste (2002).

[1] J. Okabayashi *et al.*, Phys. Rev. B **58**, R4211 (1998).
[2] J. Okabayashi *et al.*, Phys. Rev. B **64**, 125304 (2001).
[3] J. Okabayashi *et al.*, Phys. Rev. B **65**, 161203 (2002).
[4] T. Mizokawa *et al.*, Phys. Rev. B **65**, 085209 (2002).
[5] A. Franciosi *et al.*, Phys. Rev. B **40**, 12 009 (1989).
[6] L. Ley *et al.*, Phys. Rev. B **35**, 2839 (1987).
[7] U. Fano, Phys. Rev. **124**, 186 (1961).
[8] L. C. Davis and L. A. Feldkamp, Phys. Rev. B **15**, 2961 (1977).
[9] L. H. Tjeng *et al.*, Phys. Rev. Lett. **67**, 501 (1991).
[10] G. van der Laan *et al.*, Phys. Rev. B **46**, 7221 (1992).
[11] H. Sato *et al.*, J. Electron Spectrosc. Relat. Phenom. **88-91**, 425 (1998).
[12] L. Floreano *et al.*, Rev. Sci. Instrum. **70**, 3855 (1999).
[13] S. Katsumoto *et al.*, Mater. Sci. Eng., B **84**, 88 (2001).
[14] K. Cho *et al.*, Phys. Rev. B **63**, 155203 (2001).
[15] S. Pagliara *et al.*, Phys. Rev. B **65**, 205107 (2002).
[16] J.J. Yeh and I. Lindau, At. Data Nucl. Data Tables **35**, 1 (1985).
[17] T. Mizokawa and A. Fujimori, Phys. Rev. B **48**, 14 150 (1993).
[18] N. Happo *et al.*, Phys. Rev. B **50**, 12 211 (1994).
[19] M. Taniguchi *et al.*, Phys. Rev. B **51**, 6932 (1995).
[20] M. C. Richter *et al.*, Phys. Rev. B **63**, 205416 (2001).